Title

Response of BRAF-Mutant Melanoma to BRAF Inhibition Is Mediated by a Network of Transcriptional Regulators of Glycolysis

Journal

Cancer Discovery, 4(4)

ISSN

2159-8274

Authors

Parmenter, Tiffany J
Kleinschmidt, Margarete
Kinross, Kathryn M
et al.

Publication Date

2014-04-01

DOI

10.1158/2159-8290.cd-13-0440

Peer reviewed

Published in final edited form as:
Cancer Discov. 2014 April ; 4(4): 423–433. doi:10.1158/2159-8290.CD-13-0440.

Response of BRAF mutant melanoma to BRAF inhibition is mediated by a network of transcriptional regulators of glycolysis

Tiffany J. Parmenter[1], **Margarete Kleinschmidt**[1,2,3], **Kathryn M. Kinross**[1,2,3], **Simon T. Bond**[4], **Jason Li**[2,5], **Mohan R. Kaadige**[6], **Aparna Rao**[1], **Karen E. Sheppard**[1,2,7], **Willy Hugo**[8], **Gulietta M. Pupo**[9], **Richard B. Pearson**[2,7,10], **Sean L. McGee**[4], **Georgina V. Long**[9,11,12], **Richard A. Scolyer**[9,11,12], **Helen Rizos**[9], **Roger S. Lo**[8], **Carleen Cullinane**[2,3], **Donald E. Ayer**[6], **Antoni Ribas**[8], **Ricky W. Johnstone**[2,13], **Rodney J. Hicks**[2,14,15,16,17], and **Grant A. McArthur**[1,2,3,14,15,16,17]

[1]Molecular Oncology Laboratory, Oncogenic Signaling and Growth Control Program, Peter MacCallum Cancer Centre, East Melbourne, VIC 3002, Australia

[2]Sir Peter MacCallum Department of Oncology, The University of Melbourne, Parkville, VIC 3010, Australia

[3]Translational Research Laboratory, Cancer Therapeutics Program, Peter MacCallum Cancer Centre, East Melbourne, VIC 3002, Australia

[4]Metabolic Remodelling Laboratory, Metabolic Research Unit, School of Medicine, Deakin University, Waurn Ponds, VIC 3216, Australia

[5]Bioinformatics Core Facility, Peter MacCallum Cancer Centre, East Melbourne, VIC 3002, Australia

[6]Department of Oncological Sciences, Huntsman Cancer Institute, University of Utah, Salt Lake City, Utah 84112-5550, USA

[7]Department of Biochemistry and Molecular Biology, University of Melbourne, Parkville, VIC 3010, Australia

[8]Jonsson Comprehensive Cancer Center, University of California Los Angeles, Los Angeles, California 90095, USA

[9]Westmead Institute for Cancer Research, University of Sydney at Westmead Millennium Institute, Westmead, New South Wales 2145, Australia

Corresponding Authors: Grant McArthur, Division of Cancer Research, Peter MacCallum Cancer Centre, Locked Bag 1, A'Beckett St, Melbourne VIC 8006, AUSTRALIA, Phone: +61-3-9656-1954, Fax: +61-3-9656-3717, grant.mcarthur@petermac.org; Rodney Hicks, Department of Molecular Imaging, Peter MacCallum Cancer Centre, Locked Bag 1, A'Beckett St, Melbourne VIC 8006, AUSTRALIA, Phone: +61-3-9656-1852, Fax: +61-3-9656-1826, rod.hicks@petermac.org.

The authors have no competing financial interests to declare.

Supplementary Data for this article are available at Cancer Discovery Online (http://cancerdiscovery.aacrjournals.org/)

Author Contributions: TJP, GAM, RJH, RWJ, SLM, AR, DEA, CC, RSL HR, RAS, GVL and RBP were responsible for conceptual design of experiments. TJP, MK, KMK, MRK, STB, KES, WH, GMP and CC were responsible for data collection. SLM, DEA, HR, RSL and AR provided essential materials for experiments conducted within. All authors contributed to data analysis/interpretation and manuscript preparation. All authors have approved the final version of this manuscript.

[10]The Cancer Signalling Laboratory, Oncogenic Signaling and Growth Control Program, Peter MacCallum Cancer Centre, East Melbourne, VIC 3002, Australia

[11]Department of Tissue Pathology & Diagnostic Oncology, Royal Prince Alfred Hospital, Sydney, NSW 2050, Australia

[12]Discipline of Pathology, Sydney Medical School, The University of Sydney, Sydney NSW 2006, Australia

[13]Gene Regulation Laboratory, Cancer Therapeutics Program, Peter MacCallum Cancer Centre, East Melbourne, VIC 3002, Australia

[14]Molecular Imaging and Targeted Therapeutics Laboratory, Cancer Therapeutics Program, Peter MacCallum Cancer Centre, East Melbourne, VIC 3002, Australia

[15]Department of Medicine, St Vincent's Hospital, University of Melbourne, Fitzroy, VIC 3065, Australia

[16]Department of Cancer Imaging, Peter MacCallum Cancer Centre, East Melbourne, VIC 3002, Australia

[17]Department of Pathology, University of Melbourne, Parkville, VIC 3010, Australia

Abstract

Deregulated glucose metabolism fulfils the energetic and biosynthetic requirements for tumour growth driven by oncogenes. Because inhibition of oncogenic BRAF causes profound reductions in glucose uptake and a strong clinical benefit in BRAF mutant melanoma, we examined the role of energy metabolism in responses to BRAF inhibition. We observed pronounced and consistent decreases in glycolytic activity in BRAF mutant melanoma cells. Moreover, we identified a network of BRAF-regulated transcription factors that control glycolysis in melanoma cells. Remarkably, this network of transcription factors, including HIF1α, c-Myc and MondoA, drives glycolysis downstream of $BRAF^{V600}$, is critical for responses to BRAF inhibition and is modulated by BRAF inhibition in clinical melanoma specimens. Furthermore, we show that concurrent inhibition of BRAF and glycolysis induces cell death in BRAF inhibitor-resistant melanoma cells. Thus, we provide a proof of principle for treatment of melanoma with combinations of BRAF inhibitors and glycolysis inhibitors.

Keywords

BRAF; melanoma; metabolism; vemurafenib; glycolysis

Introduction

Increased glycolysis in tumour cells compared to normal tissues is observed in most cancers and supports the increased energetic and biosynthetic demands of tumour cells (1). Control of glycolysis by oncogenes and tumour suppressors such as AKT, p53 and c-Myc is believed to contribute to their tumourigenic activities (2). Treatment of AKT-driven tumour cells or tumours with PI3K/AKT/mTOR inhibitors such as PF04691502, BEZ235 and ridaforolimus suppresses glucose uptake and tumour growth/cell survival (3-5). While the role of glucose

metabolism in oncogene-driven tumourigenesis has been well characterized, it remains unclear whether regulation of glucose metabolism by oncogenes is important for tumour responses to oncogene-targeted therapy.

The development of therapies targeting BRAF in melanoma is a clear example of successful targeting of an oncogene for the treatment of cancer. Activating BRAF mutations, particularly the V600 amino acid substitution, have been identified in approximately 50% of metastatic melanomas (6) and $BRAF^{V600}$ melanomas rely on RAF/MEK/ERK signalling for growth and survival (7). $BRAF^{V600}$ expression has been associated with increased glycolytic activity and cell surface glucose transporter 1 (GLUT1) expression in colorectal and thyroid cancer cells (8, 9), indicating that glucose metabolism could be important for BRAF-driven tumourigenesis. Recently, RAF/MEK/ERK pathway inhibitors, including the BRAF inhibitors (BRAFi) vemurafenib (RG7204; PLX4032) and dabrafenib (GSK2118436), have been validated for treatment of $BRAF^{V600}$ melanoma, with striking response rates in excess of 50% in patients diagnosed with $BRAF^{V600}$ metastatic melanoma (10-14). Importantly, $BRAF^{V600}$ inhibition potently suppresses uptake of the radioactive glucose tracer 2-deoxy-2-(^{18}F)fluoro-D-glucose (FDG) in $BRAF^{V600}$ human melanoma cells and xenografts (15, 16) and in $BRAF^{V600}$ melanoma patients (10, 17, 18), suggesting that inhibition of glycolysis by BRAF pathway inhibition could be important for clinical responses to BRAFi.

Here, we show that BRAFi potently suppressed glycolysis independently of cell cycle progression and cell death via suppression of hexokinase II (HK2) and glucose transporter-1 and -3 (GLUT1/3) expression in melanoma cells and in clinical $BRAF^{V600}$ melanomas biopsies. We also found that glucose metabolism is restored upon development of BRAFi resistance, a major challenge in the clinical management of $BRAF^{V600}$ melanoma, and that this is overcome by combination with a glycolysis inhibitor. We used microarray experiments to elucidate the mechanisms by which RAF/MEK/ERK signalling promotes glycolysis. This led us to identify and validate a novel network of transcriptional regulators of glycolysis, comprised of HIF1α, c-Myc and MondoA that are altered by BRAFi treatment and development of BRAF inhibitor resistance in $BRAF^{V600}$ melanoma cells and in $BRAF^{V600}$ melanoma biopsies.

Results

To determine the effect of RAF/MEK/ERK signalling on glucose metabolism in melanoma cells, a panel of $BRAF^{WT}$ and $BRAF^{V600}$ human melanoma cells were treated with the BRAF inhibitor, vemurafenib. As expected, vemurafenib suppressed [^{3}H]-2DOG uptake (a surrogate marker of glycolytic flux) in $BRAF^{V600}$ but not $BRAF^{WT}$ melanoma cells (Fig. 1A). Furthermore, the degree to which vemurafenib inhibited glucose uptake correlated significantly with the degree of sensitivity to vemurafenib-mediated suppression of proliferation (r^2=0.7355; p=0.0002; Fig. 1B). Furthermore, we show that the degree of glycolysis suppression significantly correlates with the degree of inhibition of the transcription of ERK target genes described herein (Fig. S1). This indicates that the degree of ERK pathway inhibition may correlate with the degree of glycolysis inhibition. Treatment with vemurafenib also suppressed lactate and ATP production in $BRAF^{V600}$ but not

$BRAF^{WT}$ cells (Fig. 1C and D), confirming that BRAFi suppresses glycolytic flux. Importantly, inhibition of glycolysis by BRAFi was not a consequence of altered cell cycle progression or apoptosis induction (Fig. S2A-D), indicating that $BRAF^{V600}$ directly promotes glycolysis in human melanoma cells. We also examined glycolytic flux and oxidative phosphorylation (oxphos) determined by measurement of the extracellular acidification rates (ECAR) and oxygen consumption rates (OCR), respectively, in melanoma cells (Fig. S3A-F). This demonstrated significant decreases in ECAR (Fig. 1E) and small decreases in OCR (Fig. 1F) in $BRAF^{V600}$ cells.

To investigate the molecular mechanisms underlying $BRAF^{V600}$-driven glycolysis, we examined the effect of BRAFi on glycolytic enzymes (Fig. S4). BRAFi increased pyruvate dehydrogenase catalytic subunit E1α (PDHE1α) phosphorylation at Ser293 which would correspond to decreased enzymatic activity and suppressed oxphos (19) (Fig 1G). Interestingly, suppression of HK2 protein expression and decreased membrane expression of GLUT1 and GLUT3 (the key GLUT isoforms expressed in human melanomas (20)) was observed in $BRAF^{V600}$ melanoma cells treated with vemurafenib (Fig. 1G and H). These changes were associated with significant reductions in mRNA expression of the genes encoding HK2, GLUT1 and GLUT3 (*HK2*, *SLC2A1* and *SLC2A3*, respectively) (Fig. 1I), indicating that $BRAF^{V600}$-mediated glycolysis regulation occurs at a transcriptional level.

To examine the effect of BRAF inhibition on markers of glycolysis in a clinical context, we analysed HK2, GLUT1 and GLUT3 mRNA expression in melanoma biopsies from patients diagnosed with $BRAF^{V600}$ melanoma obtained prior to treatment (Pre), early on treatment (EOT) with a BRAFi (Day 3-22) and after disease progression (Prog; Table S1). In most cases, expression of the *HK2*, *SLC2A1* and *SLC2A3* genes significantly decreased upon BRAFi treatment ($p<0.05$) and was significantly restored upon development of drug resistance (Fig. 1J; Fig. S5A-F). Biopsies from patients that experienced stable disease or a partial response to BRAFi (RECIST criteria) demonstrated significantly greater reductions in tumour SLC2A1 mRNA levels compared to patients that experienced disease progression (Fig. 1K; $p=0.04$). This agrees with the potent suppression of FDG uptake in $BRAF^{V600}$ melanomas after BRAFi therapy (10, 17, 18). Based on these data, we hypothesised that melanoma cells require glycolysis for proliferation/survival. Consistent with this hypothesis, inhibition of glycolysis via siRNA-mediated knockdown of HK2, GLUT1 or GLUT3 or glucose withdrawal suppressed the proliferation of human melanoma cell lines (Fig. S6A-D).

Acquired resistance to BRAF inhibition occurs clinically after a median of 5-8 months (14, 21) and several mechanisms of resistance have been identified, including activation of NRAS (22). Based on the clinical importance of BRAFi resistance and the observation that HK2 and GLUT1/3 mRNA expression is restored in some patient tumours upon disease progression (Fig. 1J), we interrogated the role of glycolysis in BRAFi resistance. We rendered $BRAF^{V600}$ melanoma cells resistant to vemurafenib by expression of activated NRAS ($NRAS^{Q61K}$), a clinically validated mechanism of acquired BRAFi resistance that restores MEK/ERK signalling (22) (Fig. S7A). $NRAS^{Q61K}$ not only restored cell proliferation (Fig. 2A), but also glucose uptake, glycolytic flux, HK2 and GLUT1/3 expression (Fig. 2B-E) in vemurafenib-treated $BRAF^{V600}$ melanoma cells. To determine

whether the dependence of melanoma cells on glucose metabolism could be exploited to overcome BRAFi resistance, we treated $BRAF^{V600}$ melanoma cells expressing $NRAS^{Q61K}$ with vemurafenib alone or in combination with the pyruvate mimetic, dichloroacetate (DCA). DCA inhibits pyruvate dehydrogenase kinase (PDK) isoforms that causes downstream reactivation of the catalytic subunit of pyruvate dehydrogenase (PDHE1α), thereby suppressing glycolytic metabolism (19).

This combination was assessed using engineered $NRAS^{Q61K}$-expressing cell lines, M249-AR4 cells that developed an NRAS mutation during long term selection in vemurafenib and an early passage cell line (M376) derived from a clinical melanoma specimen with acquired vemurafenib resistance that developed an NRAS mutation (22). Inhibition of PDK using a concentration of DCA that almost completely suppresses PDHE1α phosphorylation produced 21.8% cell death in A375 $BRAF^{V600}$ melanoma cells (Fig. S7B-C). However, combination treatment with vemurafenib + DCA induced apoptosis to a greater degree than either agent alone (Fig. 2F; Fig. S7D) concomitant with greater inhibition of lactate/ATP production (Fig. 2G; Fig. S7E-F). We also observed a significant, albeit less pronounced, enhancement of the effect of the MEK inhibitor PD0325901 (PD901) by DCA on vemurafenib-resistant melanoma cells, indicating that the extent of ERK inhibition is likely to be important for the enhancement produced by glycolysis inhibition (Fig. S8).

Combination treatment of vemurafenib-resistant melanoma cells did not enhance the suppression of ERK or PDHE1α phosphorylation by vemurafenib or DCA alone, indicating that the interaction between these drugs doesn't result from enhancement of drug activity (Fig. 2H, Fig S7G). As expected, 1h or 20h of treatment with vemurafenib + DCA increased the basal OCR and decreased the basal ECAR of vemurafenib-resistant melanoma cells, respectively (Fig. 2I-J, Fig. S9A-D), indicating that vemurafenib + DCA treatment causes reentry of pyruvate into the TCA cycle and increases oxphos resulting in suppressed glycolytic metabolism. Intriguingly, vemurafenib + DCA treatment for 1h increased uncoupled respiration in vemurafenib-resistant cells (Fig. 2I, Fig. S9A-D), suggesting that oxphos has become dysfunctional in these cells. In support of this hypothesis, 20h of treatment with vemurafenib + DCA potently suppressed the basal OCR and ATP turnover of vemurafenib-resistant cells (Fig. 2J, Fig. S9A-D). Furthermore, vemurafenib + DCA potently increased superoxide production and TMRE staining (indicative of mitochondrial hyperpolarisation) in vemurafenib-resistant cells (Fig. 2K, Fig. S7H).

Initially, we examined the possible involvement of mTOR in glycolytic responses to BRAF inhibition, as mTOR complex 1 (mTORC1) activity has been shown to be important for responses to BRAF inhibition in melanoma (23) and may also be important for Akt-driven glycolysis. We found that after 2h of treatment with vemurafenib, ribosomal protein S6 phosphorylation was modestly suppressed, but that 4EBP1 phosphorylation was unchanged. These observations could be explained by mTORC1-dependent regulation of S6 by ERK, although mTORC1-independent regulation of S6 by ERK as has also been described (24). After 24h of treatment, stronger inhibition of S6 and 4EBP1 phosphorylation occurred (Fig. S10). Because glucose uptake is maximally suppressed within 20h of vemurafenib treatment, and because significant inhibition of GLUT1, and GLUT3 mRNA expression occurs within 4h of vemurafenib treatment (Fig. S10) it is unlikely these late changes to

mTORC1 activity contribute significantly to the regulation of glycolysis by vemurafenib. Previous work has also demonstrated that $BRAF^{V600}$ regulates LKB1/AMPK pathway activity in melanoma cells (25). Because this pathway is known to regulate energy metabolism, we examined its involvement in $BRAF^{V600}$-driven glycolysis. We did not observe consistent regulation of LKB1/AMPK signalling by vemurafenib in melanoma cells (Fig. S10). Thus, $BRAF^{V600}$-mediated regulation of glycolysis in melanoma cells occurs by an as yet unidentified mechanism. To investigate the mechanism by which $BRAF^{V600}$ regulates glycolysis in melanoma, we conducted microarrays and used gene set enrichment analysis (GSEA) and candidate gene analysis to identify putative glycolysis-regulating BRAF targets.

Of the gene sets that were significantly enriched in control versus vemurafenib-treated cells (Supplementary datasets 1, 2), we identified 15 c-Myc-regulated and 4 hypoxia-regulated gene sets as well as 3 glycolysis-related gene sets (Fig. 3A, Table S2). Because c-Myc and HIF1α (the key mediator of hypoxia-stimulated gene transcription) are established positive regulators of glucose metabolism (26, 27), we posited that these are likely to be important for regulation of glycolysis by $BRAF^{V600}$. MondoA, however, is a critical negative regulator of glucose uptake (28). Although regulation of energy metabolism and the regulation of MondoA activity by oncogenic signalling pathways is well-defined (28), the role of MondoA in tumourigenesis has yet to be fully elucidated. Here, we describe significant increases in expression of thioredoxin interacting protein (TXNIP) and arrestin domain containing 4 (ARRDC4), two direct transcriptional targets of MondoA (28), in response to BRAF inhibition (Fig. 3B) demonstrating that MondoA is negatively regulated by $BRAF^{V600E}$. To confirm this, we performed ChIP assays to examine binding of MondoA to the TXNIP and ARRDC4 promoters and observed that vemurafenib treatment stimulated binding of MondoA to both the TXNIP and ARRDC4 promoters in vemurafenib sensitive A375-pBp (Fig. 3C). Importantly, $NRAS^{Q61K}$ expression suppressed this effect, indicating tight regulation of MondoA promoter binding activity by mutant BRAF.

We confirmed that vemurafenib treatment increased TXNIP expression and decreased c-Myc and HIF1α expression at the mRNA and protein levels in $BRAF^{V600}$ melanoma cell lines (Fig. 3D and E). Interestingly, BRAFi did not alter total MondoA protein expression (Fig. 3E), indicating that $BRAF^{V600}$ regulates the association of MondoA with target gene promoters. To examine the mechanism of regulation of c-Myc and HIF1α expression, we co-treated melanoma cells with vemurafenib and the proteasome inhibitor, bortezomib. Bortezomib limited the effect of vemurafenib on HIF1α protein expression, thus, $BRAF^{V600}$ suppresses c-Myc and HIF1α transcription and HIF1α degradation (Fig. S10). Importantly, we confirmed altered expression of these transcription factors in clinical melanoma specimens after BRAFi treatment. Although overall changes in HIF1α and c-Myc expression did not reach statistical significance, their expression was clearly decreased EOT and restored after progression in a subset of patient biopsies. In the cases of c-Myc and HIF1α, regional microenvironmental and hypoxic variability would significantly affect gene expression, making it difficult gain an accurate representation of mRNA expression from a small biopsy. We also observed that TXNIP mRNA expression was consistently and significantly increased from baseline during treatment with a BRAF inhibitor (p=0.002) and

decreased compared to on-treatment expression levels (p=0.016) after disease progression. (Fig 3F; Fig. S5A-F). Moreover, biopsies from patients that experienced stable disease or a partial response to BRAFi (RECIST criteria) demonstrated significantly greater increases in TXNIP mRNA levels compared to biopsies from patients that experienced disease progression (Fig 3G; p=0.02), indicating the potential importance of TXNIP for responses to BRAF inhibition.

To examine regulation of glucose metabolism by MondoA, c-Myc and HIF1α directly, each transcriptional regulator was targeted with siRNAs. Knockdown of c-Myc or HIF1α phenocopied the inhibitory effect of BRAF knockdown on glucose uptake and cell proliferation while MondoA knockdown significantly increased basal glucose uptake in melanoma cells (Fig. 4A-C). This confirms that c-Myc and HIF1α promote glucose uptake, while MondoA suppresses basal glucose uptake in $BRAF^{V600}$ melanoma cells. Inhibition of gene expression using siRNAs showed that MondoA suppresses basal GLUT1 and GLUT3 expression, HIF1α promotes basal GLUT1 expression and c-Myc promotes basal GLUT1 and HK2 expression while suppressing GLUT3 suppression (Fig 4D), demonstrating that each of these transcription factors controls a different subset of glycolytic targets. To address the role of this BRAF-regulated transcriptional network in responses to vemurafenib, we functionally modulated network components and examined the impact on vemurafenib responses. Suppression of glycolysis and cell proliferation by vemurafenib was partially reversed by siRNA-mediated MondoA knockdown, activation of inducible c-Myc (MycER) or by exposure to hypoxia (that causes HIF1α stabilization) in $BRAF^{V600}$ melanoma cells (Fig. 4E-M). This involved restored GLUT1/3 expression after siRNA-mediated MondoA knockdown, GLUT1 expression by hypoxia and HK2/GLUT1 expression by c-Myc overexpression in the presence of vemurafenib in WM266.4 $BRAF^{V600}$ melanoma cells.

Discussion

Recent reports have shown a link between $BRAF^{V600}$ and glycolysis in both *in vitro* and *in vivo* models of cancer and in a clinical setting (8, 9, 12, 17, 21). Importantly, BRAFi has been shown to suppress glucose uptake in melanoma cells and xenografts (13, 16) and in patient tumours (10, 15, 17, 18). Here, we show that vemurafenib suppresses glycolysis in $BRAF^{V600}$ melanoma cells independently of cell cycle progression or cell death. In some cases, small reductions in the rate of oxphos occur in response to vemurafenib, however these changes are only very modest and do not occur in all vemurafenib cell lines. Conversely, inhibition of glucose uptake significantly correlated with vemurafenib sensitivity, indicating that the degree of ERK pathway output profoundly influences the magnitude of glucose uptake in melanoma cells. Expression of HK2 and GLUT1/3 was significantly and consistently decreased in $BRAF^{V600}$ melanoma cells in response to BRAF inhibition and this is likely to underlie vemurafenib -mediated suppression of glycolysis. Consistent with a role for glycolysis in cell survival, we describe dependence on glucose availability and expression of the glycolytic machinery for melanoma cell proliferation. Importantly, expression of GLUT1, GLUT3 or HK2 mRNA was suppressed in melanoma biopsies from patients treated with the BRAFi dabrafenib or vemurafenib and, in some cases, was restored after disease progression. Thus, our data significantly expands on the

current understanding of $BRAF^{V600}$-driven glucose metabolism and suggests a possible role for glycolysis in responses and resistance of melanoma to BRAF-targeted therapies.

Based on the restoration of GLUT1/3 or HK2 mRNA expression in some patient biopsies, we examined glycolysis in vemurafenib-resistant melanoma cells. Resistance to vemurafenib develops clinically after a median of 5-8 months (14, 21) and poses a significant challenge for the clinical management of $BRAF^{V600}$ melanoma. Vemurafenib-resistant melanoma cells exhibited restored MEK/ERK activation, cell proliferation, HK2 and GLUT1/3 expression and glucose uptake. Therefore, we determined whether the dependency of melanoma cells on glycolysis could be exploited to overcome vemurafenib resistance. We used the PDK inhibitor, DCA, that causes downstream reactivation of PDHE1α, thereby increasing pyruvate entry into the mitochondrial citric acid cycle/oxphos and suppressing glycolysis (19). DCA restored vemurafenib sensitivity in melanoma cells that display BRAF inhibitor resistance via NRAS activation. This agrees with a recent study demonstrating that shRNAs targeting PDK1 synergise with BRAF inhibition in transformed human melanocytes and melanoma cells to suppress cell survival (29). We build on these observations, demonstrating potent induction of ROS production and mitochondrial hyperpolarisation after treatment with vemurafenib + a PDK inhibitor, indicating that mitochondrial dysfunction resulting from combination treatment. Because generation of ROS and mitochondrial hyperpolarisation can precede apoptotic cell death (30), we hypothesise that these factors underlie the synergistic induction of cell death by combined BRAF and PDK inhibition. A recent study investigated the possible use of DCA for treatment of glioblastoma and, despite some positive results, dose-dependent toxicities limited the application of this inhibitor. Further development of more specific inhibitors of PDK1 with more favourable pharmacokinetic profiles and fewer toxicities is currently underway (29)

To investigate the mechanism by which $BRAF^{V600}$ regulates glycolysis, we conducted gene expression arrays to identify putative glycolysis-regulating BRAF targets. We identified a network of transcription factors, including MondoA, HIF1α and c-Myc, which is tightly regulated by $BRAF^{V600}$. Expression of these transcription factors is altered by vemurafenib treatment in $BRAF^{V600}$ melanoma cells and, importantly, in clinical melanoma specimens. Notably, the consistent modulation of TXNIP expression after BRAF inhibitor treatment and disease progression in melanoma biopsies indicates that MondoA is a therapeutically important target of mutant BRAF that is likely to play an important role in the suppression of FDG uptake in the context of BRAF mutant melanoma observed in patients.

We have also established the functional importance of this transcriptional network for $BRAF^{V600}$-driven glycolysis and melanoma cell proliferation. Stabilization of HIF1α and upregulation of c-Myc expression has been demonstrated in a huge range of cancers, including melanomas, and regulation of HIF1α and c-Myc expression by the RAF/MEK/ERK pathway has been previously described (31, 32). We found that expression of c-Myc and HIF1α is required for maintenance of basal glucose uptake in melanoma cells. Conversely, although regulation of MondoA by oncogenic signalling pathways has been established (28), the role of MondoA in tumourigenesis is unclear. We show for the first time that MondoA is regulated by $BRAF^{V600}$ and suppresses basal glucose uptake in

melanoma cells. Furthermore, inhibition of c-Myc and HIF1α and activation of MondoA suppression is critical for metabolic and proliferative responses to vemurafenib.

Recently, Kaplon and colleagues (29) demonstrated that pyruvate dehydrogenase (PDH) is critical for oncogene induced senescence (OIS) induced by $BRAF^{V600E}$ in mouse melanocytes and that abrogation of PDH activity overcame $BRAF^{V600E}$-induced OIS. This agrees with our observation that BRAF inhibition suppresses PDH activity in BRAF mutant melanoma cells (evidenced by increased PDH phosphorylation). These observations suggest that regulation of energy metabolism plays a pivotal role important for tumour development, cell survival and BRAF inhibitor responses in the context of BRAF mutant melanoma.

Our findings show striking reductions in glycolysis and small reductions in the rate of oxygen consumption as an early response to BRAFi (24h treatment). A recent study published by Haq *et al.* (33) examining later time points (72h treatment) and adaptation to BRAFi, demonstrated increased mitochondrial biogenesis and expression of oxphos genes in BRAFi treated melanoma cells that was associated with increased PGC1α expression. These data are consistent with a model of early treatment response wherein potent inhibition of ERK/MAPK pathway activity suppresses glycolysis followed by longer-term adaptive changes including increased oxphos in cells surviving BRAF inhibition. Long-term BRAF inhibition and stimulation of oxphos associated with increased mitochondrial activity might occur as a mechanism to overcome the suppression of glycolysis by BRAF inhibition described herein. Consistent with this suggestion, Gopal *et al.* found that melanoma cell lines displaying *de novo* resistance to ERK/MAPK pathway inhibition have a high basal rate of oxphos and increased expression of oxphos genes compared to MEK inhibitor-sensitive cell lines and that this is associated with high expression of PGC1α (Y. Gopal and M. Davies personal communication). Taken together, these findings indicate that sensitivity to ERK/MAPK pathway inhibitors in the context of melanoma may be defined by a reliance on glycolysis for survival and that stimulation of oxphos by ERK/MAPK pathway inhibition or high basal oxphos are associated with *de novo* and early adaptation and acquired resistance to ERK/MAPK pathway inhibition. Together these data suggest that the metabolic background of a BRAF mutant melanoma could be pivotal for responses to BRAF inhibition.

In summary, we have demonstrated that mutant BRAF tightly regulates glycolysis independently of cell cycle progression or cell death and show that melanoma cells have a requirement for access to glucose and intact glycolytic machinery for their proliferation. Combination of vemurafenib with the glycolytic inhibitor DCA was shown to restore sensitivity to BRAF inhibition in NRAS-activated vemurafenib -resistant melanoma cells, not only demonstrating the importance of glycolysis for melanoma cell survival but also providing a proof of principle for the combination of targeted therapeutics such as vemurafenib with glycolysis inhibitors to prevent the emergence of drug resistance. Finally, we have identified a network of glycolysis regulators that operate under the control of oncogenic $BRAF^{V600}$ to modulate glucose uptake in melanoma cells and are altered in clinical melanoma biopsies early during BRAFi treatment and upon development of resistance to BRAFi. For the first time, our data show that inhibition of glycolysis via this

network is critical for the suppression of proliferation and glucose uptake induced by inhibition of oncogenic BRAF.

Methods

See online supplementary materials for a full description of methods.

Materials and Cells

Vem and its analog PLX4720 were provided by Plexxikon Inc. (Berkeley, CA, USA). Sodium dichloroacetate (DCA) was purchased from Sigma-Aldrich. PD-0332991 (PD991) provided by Pfizer Inc. HEK-293T, MALME-3M, COLO829, A375, SK-MEL-28, HT144, LOX-IMVI, SK-MEL-2, A2058, CHL1 and MeWo cells were purchased from the American Tissue Culture Collection (ATCC) and National Cancer Institute (NCI). CO89 and D04-M1 cells were obtained from the Australasian Biospecimen Network-Oncology Cell Line Bank at the QIMR. Individuality of the melanoma cell lines was confirmed on early passage cells by PCR based short tandem repeat (STR) analysis using six STR loci and this analysis was routinely performed to confirm the identity of cell lines. M249, M249-AR4 and M376 were a gift from Dr. Antoni Ribas (Department of Molecular and Medical Pharmacology, David Geffen School of Medicine, University of California, Los Angeles). All melanoma cell lines were maintained in RPMI 1640 containing 10% FBS, 2 mM L-alanyl-L-glutamine, 1% penicillin/streptomycin and 250 ng/ml amphotericin B in a 37°C humidified, 5% CO_2 incubator. The BRAF and NRAS mutation status of all cell lines has been reported previously (34, 35) and is described in table S3. M249-AR4 and M376 cells were maintained as above with the addition of 1μM Vem. HEK-293T cells were cultured in DMEM containing 10% FBS, 2 mM L-alanyl-L-glutamine, 1% penicillin/streptomycin and 250 ng/ml amphotericin B in a 37°C humidified, 5% CO_2 incubator. Melanoma cell lines with a vemurafenib IC50 (determined by SRB assays; table S3) of greater than 1μM were considered to be vemurafenib-resistant. The M249 cell line is a $BRAF^{V600E}$ cell line while the M249-AR4 cell line was derived from M249 cells by long-term culture in Vem and was shown to have developed an NRAS mutation (22). The M376 cell line was derived from a patient tumour after relapse on Vem therapy and was also shown to harbour an NRAS mutation (22).

Analysis of bioenergetics using the Seahorse XF24 extracellular flux analyser—All extracellular flux analyses were performed using the Seahorse XF24 Extracellular Flux Analyser (Seahorse Bioscience, Billerica, USA). 24 well Seahorse V7 plates were seeded at 5×10^4 cells/well, and 24h later the cells were treated with either 1) vehicle, vemurafenib (3 μM) for 20 hours, or 2) Vehicle, vemurafenib (15μM), DCA (20mM), vemurafenib + DCA in combination for 1h or 20h. ECAR and OCR were determined simultaneously (see supplementary methods for a full description).

Microarray experiments

A375 $BRAF^{V600E}$ human melanoma cells were treated with 3 μM vemurafenib or vehicle (0.1% DMSO) for 24h after which RNA was extracted (n=3). Whole-transcript sense target preparation and labelling (using the GeneChip® WT Terminal Labelling and Controls and

Ambion® WT Expression Kits), hybridization to Affymetrix GeneChip® 1.0 ST human gene arrays and array scanning were completed by The Ramaciotti Centre Microarray Service, University of New South Wales, New South Wales, Australia. Data analysis is described in the Supplementary Methods. Melanoma cell line microarray data have been deposited in The Gene Expression Omnibus of the National Center for Biotechnical Information (accession number GSE42872).

Supplementary Material

Refer to Web version on PubMed Central for supplementary material.

Acknowledgments

We would like to acknowledge Stand Up To Cancer, Burroughs Wellcome Fund, Melanoma Research Alliance, American Skin Association, Harry J. Lloyd Charitable Trust and The Seaver Institute. We thank Kaylene Simpson and staff at the Victorian Centre for Functional Genomics (VCFG) for guidance in the design of siRNA-based experiments. We acknowledge Gideon Bollag and Plexxikon/Roche for providing vemurafenib (PLX4032) and PLX4720. We also thank Megan Bywater, Andreas Möeller, Jaclyn Sceneay, Gretchen Poortinga, Elaine Sanij, Jeannine Diesch, Kate Hannan, Kerry Ardley, Rachel Walker, Ross Hannan and Ralph Rossi for technical assistance and conceptual input. The Ramaciotti Centre for Gene Function Analysis, UNSW, Sydney, Australia, assisted with microarrays. Support from the staff at the Melnanoma Institute, Australia is also gratefully acknowledged.

Financial support. This work was supported by grants from the National Health and Medical Research Council of Australia to RJH, AR, RAS and GAM, Cancer Council Victoria to RJH and GAM, the Cancer Institute New South Wales to RAS, HR and GVL, NCI K22CA151638 and 1P01CA168585 to RSL and NIH R01055668 to DEA. GAM was a recipient of the Sir Edward Dunlop Fellowship of the Cancer Council of Victoria. SLM is supported by an NHMRC Career Development Fellowship (APP1030474).

References

1. Vander Heiden MG, Cantley LC, Thompson CB. Understanding the Warburg effect: the metabolic requirements of cell proliferation. Science. 2009; 324(5930):1029–33. Epub 2009/05/23. doi: 324/5930/1029 [pii]. 10.1126/science.1160809 [PubMed: 19460998]
2. Levine AJ, Puzio-Kuter AM. The control of the metabolic switch in cancers by oncogenes and tumor suppressor genes. Science. 2010; 330(6009):1340–4. Epub 2010/12/04. doi: 330/6009/1340 [pii]. 10.1126/science.1193494 [PubMed: 21127244]
3. Engelman JA, Chen L, Tan X, Crosby K, Guimaraes AR, Upadhyay R, et al. Effective use of PI3K and MEK inhibitors to treat mutant Kras G12D and PIK3CA H1047R murine lung cancers. Nat Med. 2008; 14(12):1351–6. Epub 2008/11/26. doi: nm.1890 [pii]. 10.1038/nm.1890 [PubMed: 19029981]
4. Kinross KM, Brown DV, Kleinschmidt M, Jackson S, Christensen J, Cullinane C, et al. In vivo activity of combined PI3K/mTOR and MEK inhibition in a Kras(G12D);Pten deletion mouse model of ovarian cancer. Mol Cancer Ther. 2011; 10(8):1440–9. Epub 2011/06/03. doi: 1535-7163.MCT-11-0240 [pii]. 10.1158/1535-7163.MCT-11-0240 [PubMed: 21632463]
5. Rivera VM, Squillace RM, Miller D, Berk L, Wardwell SD, Ning Y, et al. Ridaforolimus (AP23573; MK-8669), a potent mTOR inhibitor, has broad antitumor activity and can be optimally administered using intermittent dosing regimens. Mol Cancer Ther. 2011; 10(6):1059–71. Epub 2011/04/13. doi: 1535-7163.MCT-10-0792 [pii]. 10.1158/1535-7163.MCT-10-0792 [PubMed: 21482695]
6. Davies H, Bignell GR, Cox C, Stephens P, Edkins S, Clegg S, et al. Mutations of the BRAF gene in human cancer. Nature. 2002; 417(6892):949–54. Epub 2002/06/18. nature00766 [pii]. 10.1038/nature00766 [PubMed: 12068308]
7. Gray-Schopfer VC, da Rocha Dias S, Marais R. The role of B-RAF in melanoma. Cancer Metastasis Rev. 2005; 24(1):165–83. Epub 2005/03/24. 10.1007/s10555-005-5865-1 [PubMed: 15785879]

8. Yun J, Rago C, Cheong I, Pagliarini R, Angenendt P, Rajagopalan H, et al. Glucose deprivation contributes to the development of KRAS pathway mutations in tumor cells. Science. 2009; 325(5947):1555–9. Epub 2009/08/08. doi: 1174229 [pii]. 10.1126/science.1174229 [PubMed: 19661383]
9. Lee MH, Lee SE, Kim DW, Ryu MJ, Kim SJ, Kim YK, et al. Mitochondrial localization and regulation of BRAFV600E in thyroid cancer: a clinically used RAF inhibitor is unable to block the mitochondrial activities of BRAFV600E. J Clin Endocrinol Metab. 2011; 96(1):E19–30. Epub 2010/10/12. doi: jc.2010-1071 [pii]. 10.1210/jc.2010-1071 [PubMed: 20926530]
10. Bollag G, Hirth P, Tsai J, Zhang J, Ibrahim PN, Cho H, et al. Clinical efficacy of a RAF inhibitor needs broad target blockade in BRAF-mutant melanoma. Nature. 2010; 467(7315):596–9. Epub 2010/09/09. doi: nature09454 [pii]. 10.1038/nature09454 [PubMed: 20823850]
11. Flaherty KT, Infante JR, Daud A, Gonzalez R, Kefford RF, Sosman J, et al. Combined BRAF and MEK inhibition in melanoma with BRAF V600 mutations. N Engl J Med. 2012; 367(18):1694–703. Epub 2012/10/02. 10.1056/NEJMoa1210093 [PubMed: 23020132]
12. Flaherty KT, Puzanov I, Kim KB, Ribas A, McArthur GA, Sosman JA, et al. Inhibition of mutated, activated BRAF in metastatic melanoma. N Engl J Med. 2010; 363(9):809–19. Epub 2010/09/08. 10.1056/NEJMoa1002011 [PubMed: 20818844]
13. Yang H, Higgins B, Kolinsky K, Packman K, Go Z, Iyer R, et al. RG7204 (PLX4032), a selective BRAFV600E inhibitor, displays potent antitumor activity in preclinical melanoma models. Cancer Res. 2010; 70(13):5518–27. Epub 2010/06/17. doi: 0008-5472.CAN-10-0646 [pii]. 10.1158/0008-5472.CAN-10-0646 [PubMed: 20551065]
14. Hauschild A, Grob JJ, Demidov LV, Jouary T, Gutzmer R, Millward M, et al. Dabrafenib in BRAF-mutated metastatic melanoma: a multicentre, open-label, phase 3 randomised controlled trial. Lancet. 2012; 380(9839):358–65. Epub 2012/06/28. 10.1016/s0140-6736(12)60868-x [PubMed: 22735384]
15. Baudy AR, Dogan T, Flores-Mercado JE, Hoeflich KP, Su F, van Bruggen N, et al. FDG-PET is a good biomarker of both early response and acquired resistance in BRAFV600 mutant melanomas treated with vemurafenib and the MEK inhibitor GDC-0973. EJNMMI Res. 2012; 2(1):22. Epub 2012/06/02. doi: 2191-219X-2-22 [pii]. 10.1186/2191-219X-2-22 [PubMed: 22651703]
16. Sondergaard JN, Nazarian R, Wang Q, Guo D, Hsueh T, Mok S, et al. Differential sensitivity of melanoma cell lines with BRAFV600E mutation to the specific Raf inhibitor PLX4032. J Transl Med. 2010; 8:39. Epub 2010/04/22. doi: 1479-5876-8-39 [pii]. 10.1186/1479-5876-8-39 [PubMed: 20406486]
17. McArthur GA, Puzanov I, Amaravadi R, Ribas A, Chapman P, Kim KB, et al. Marked, homogeneous, and early [18F]fluorodeoxyglucose-positron emission tomography responses to vemurafenib in BRAF-mutant advanced melanoma. J Clin Oncol. 2012; 30(14):1628–34. Epub 2012/03/29. doi: JCO.2011.39.1938 [pii]. 10.1200/JCO.2011.39.1938 [PubMed: 22454415]
18. Carlino MS, Saunders CA, Haydu LE, Menzies AM, Martin Curtis C Jr, Lebowitz PF, et al. (18)F-labelled fluorodeoxyglucose-positron emission tomography (FDG-PET) heterogeneity of response is prognostic in dabrafenib treated BRAF mutant metastatic melanoma. European journal of cancer (Oxford, England : 1990). 2013; 49(2):395–402. Epub 2012/09/18. 10.1016/j.ejca.2012.08.018 [PubMed: 22981500]
19. Papandreou I, Goliasova T, Denko NC. Anticancer drugs that target metabolism: Is dichloroacetate the new paradigm? Int J Cancer. 2011; 128(5):1001–8. Epub 2010/10/20. 10.1002/ijc.25728 [PubMed: 20957634]
20. Parente P, Coli A, Massi G, Mangoni A, Fabrizi MM, Bigotti G. Immunohistochemical expression of the glucose transporters Glut-1 and Glut-3 in human malignant melanomas and benign melanocytic lesions. J Exp Clin Cancer Res. 2008; 27:34. Epub 2008/09/04. doi: 1756-9966-27-34 [pii]. 10.1186/1756-9966-27-34 [PubMed: 18764953]
21. Chapman PB, Hauschild A, Robert C, Haanen JB, Ascierto P, Larkin J, et al. Improved survival with vemurafenib in melanoma with BRAF V600E mutation. N Engl J Med. 2011; 364(26):2507–16. Epub 2011/06/07. 10.1056/NEJMoa1103782 [PubMed: 21639808]
22. Nazarian R, Shi H, Wang Q, Kong X, Koya RC, Lee H, et al. Melanomas acquire resistance to B-RAF(V600E) inhibition by RTK or N-RAS upregulation. Nature. 2010; 468(7326):973–7. Epub 2010/11/26. doi: nature09626 [pii]. 10.1038/nature09626 [PubMed: 21107323]

23. Corcoran RB, Rothenberg SM, Hata AN, Faber AC, Piris A, Nazarian RM, et al. TORC1 suppression predicts responsiveness to RAF and MEK inhibition in BRAF-mutant melanoma. Science translational medicine. 2013; 5(196):196ra98. Epub 2013/08/02. 10.1126/scitranslmed.3005753 [PubMed: 23903755]
24. Roux PP, Shahbazian D, Vu H, Holz MK, Cohen MS, Taunton J, et al. RAS/ERK signaling promotes site-specific ribosomal protein S6 phosphorylation via RSK and stimulates cap-dependent translation. The Journal of biological chemistry. 2007; 282(19):14056–64. Epub 2007/03/16. 10.1074/jbc.M700906200 [PubMed: 17360704]
25. Zheng B, Jeong JH, Asara JM, Yuan YY, Granter SR, Chin L, et al. Oncogenic B-RAF negatively regulates the tumor suppressor LKB1 to promote melanoma cell proliferation. Mol Cell. 2009; 33(2):237–47. Epub 2009/02/04. doi: S1097-2765(09)00002-1 [pii]. 10.1016/j.molcel.2008.12.026 [PubMed: 19187764]
26. Dang CV. MYC on the path to cancer. Cell. 2012; 149(1):22–35. Epub 2012/04/03. doi: S0092-8674(12)00296-6 [pii]. 10.1016/j.cell.2012.03.003 [PubMed: 22464321]
27. Marin-Hernandez A, Gallardo-Perez JC, Ralph SJ, Rodriguez-Enriquez S, Moreno-Sanchez R. HIF-1alpha modulates energy metabolism in cancer cells by inducing over-expression of specific glycolytic isoforms. Mini Rev Med Chem. 2009; 9(9):1084–101. Epub 2009/08/20. [PubMed: 19689405]
28. Peterson CW, Ayer DE. An extended Myc network contributes to glucose homeostasis in cancer and diabetes. Front Biosci. 2011; 16:2206–23. Epub 2011/05/31. doi: 3848 [pii]. [PubMed: 21622171]
29. Kaplon J, Zheng L, Meissl K, Chaneton B, Selivanov VA, Mackay G, et al. A key role for mitochondrial gatekeeper pyruvate dehydrogenase in oncogene-induced senescence. Nature. 2013 Epub 2013/05/21. doi: nature12154[pii] doi:10.1038/nature12154 [doi] 23685455.
30. Vander Heiden MG, Chandel NS, Schumacker PT, Thompson CB. Bcl-xL prevents cell death following growth factor withdrawal by facilitating mitochondrial ATP/ADP exchange. Mol Cell. 1999; 3(2):159–67. Epub 1999/03/17. doi: S1097-2765(00)80307-X [pii]. [PubMed: 10078199]
31. Mills CN, Joshi SS, Niles RM. Expression and function of hypoxia inducible factor-1 alpha in human melanoma under non-hypoxic conditions. Mol Cancer. 2009; 8:104. Epub 2009/11/19. doi: 1476-4598-8-104 [pii] doi: 10.1186/1476-4598-8-104 [doi] 19919690 PMC2781803. [PubMed: 19919690]
32. Tsai WB, Aiba I, Long Y, Lin HK, Feun L, Savaraj N, et al. Activation of Ras/PI3K/ERK pathway induces c-Myc stabilization to upregulate argininosuccinate synthetase, leading to arginine deiminase resistance in melanoma cells. Cancer Res. 2012; 72(10):2622–33. Epub 2012/03/31. doi: 0008-5472.CAN-11-3605 [pii]. 10.1158/0008-5472.CAN-11-3605 [PubMed: 22461507]
33. Haq R, Shoag J, Andreu-Perez P, Yokoyama S, Edelman H, Rowe GC, et al. Oncogenic BRAF regulates oxidative metabolism via PGC1alpha and MITF. Cancer Cell. 2013; 23(3):302–15. Epub 2013/03/13. doi: S1535-6108(13)00067-6 [pii]. 10.1016/j.ccr.2013.02.003 [PubMed: 23477830]
34. Ikediobi ON, Davies H, Bignell G, Edkins S, Stevens C, O'Meara S, et al. Mutation analysis of 24 known cancer genes in the NCI-60 cell line set. Mol Cancer Ther. 2006; 5(11):2606–12. Epub 2006/11/08. doi: 1535-7163.MCT-06-0433 [pii]. 10.1158/1535-7163.MCT-06-0433 [PubMed: 17088437]
35. Stark M, Hayward N. Genome-wide loss of heterozygosity and copy number analysis in melanoma using high-density single-nucleotide polymorphism arrays. Cancer Res. 2007; 67(6):2632–42. Epub 2007/03/17. doi: 67/6/2632 [pii]. 10.1158/0008-5472.CAN-06-4152 [PubMed: 17363583]

Significance

BRAF inhibitors suppress glycolysis and provide strong clinical benefit in $BRAF^{V600}$ melanoma. We show that BRAF inhibition suppresses glycolysis via a network of transcription factors that are critical for complete BRAF inhibitor responses. Furthermore, we provide evidence for the clinical potential of therapies that combine BRAF inhibitors with glycolysis inhibitors.

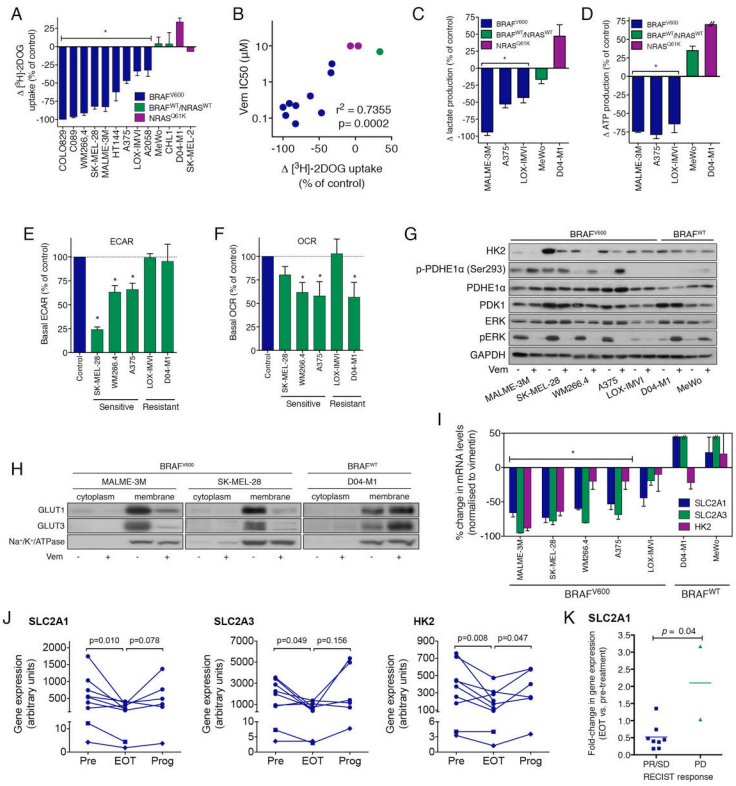

Figure 1.

BRAF^{V600E} promotes glycolysis in melanoma cells via regulation of GLUT1, GLUT3 and HK2. **A** [^{3}H]-2DOG uptake in melanoma cells (expressed as % change control vs. 3μM vemurafenib (Vem) 20h). **B** Pearson's correlation between inhibition of [^{3}H]-2DOG uptake by Vem and proliferation IC50s for Vem treatment. **C** L-Lactate production and **D** ATP production were determined in Vem-treated melanoma cells (expressed as % change; control vs. 3μM Vem 20h). **E** ECAR and **F** OCR in human melanoma cells (% of control) determined using a Seahorse XF24 Extracellular Flux Analyzer. **G** Effect of Vem on protein expression in melanoma cells was determined by Western immunoblotting (Control vs. 3μM Vem 20h) using GAPDH as a loading control. **H** Membrane vs. cytoplasmic GLUT1 and GLUT3 expression in melanoma cells (Control vs. 3μM Vem 20h). Na^+K^+ATPase was used as a membrane-specific loading control. **I** gene expression of *SLC2A1* (GLUT1), *SLC2A3* (GLUT3) and *HK2* (Control vs. 3μM Vem 20h) was determined by quantitative RT-PCR. **J** mRNA expression in melanoma biopsies. For all patients, RNA was extracted from fresh-frozen BRAF^{V600} melanoma biopsies obtained from patients pre-treatment (Pre), early on dabrafenib (BRAFi) ± trametinib (MEK inhibitor) or vemurafenib therapy (BRAFi) (EOT) and, in some cases, after disease progression (Prog). Data are included only for patients that showed stable disease or a partial response (RECIST criteria) early on treatment. Changes in gene expression were determined using an Illumina BeadStation (patients 1-7 (x025CF)), Affymetrix Human Gene 1.0 ST Arrays (patient 8 (x25C6)) or by RNAseq for patient 9 ((x025A0)). For all patients, data are expressed as the mean average signal intensity across all biopsies for an individual patient at each time point. **K** Change in SLC2A1 gene expression between baseline and early on treatment in responders (partial response (PR) or

stable disease (SD)) versus non-responders (progressive disease; PD) to BRAFi ± MEKi treatment. **A, C, D** data represent mean ± SEM (n=3). * $p<0.05$. Data were analysed using a one-way ANOVA coupled with Tukey's multiple comparison *post-hoc* test. **E, F** data represent mean ± SEM (n=5). * $p<0.05$. Data were analysed using a one-way ANOVA coupled with Tukey's multiple comparison *post-hoc* test. **B** Pearson's correlation * $p<0.05$. **I** data represent mean ± SEM (n=3). * $p<0.05$. Two-way ANOVA coupled with a Tukey's *post-hoc* test. **G & H** images are representative of 2 independent experiments. **J** Data points represent mean data values across all biopsies from a single patient pre-treatment and lines represent individual patients. Data were analysed using *t*-tests coupled with Wilcoxon's matched-pairs signed rank test and $p<0.05$ denotes a statistically significant difference. **K** Lines represent mean fold-change in gene expression (EOT vs. Pre) and symbols represent individual patients. Data were analysed using a *t*-test coupled with a Mann-Whitney test where $p<0.05$ denotes a statistically significant difference.

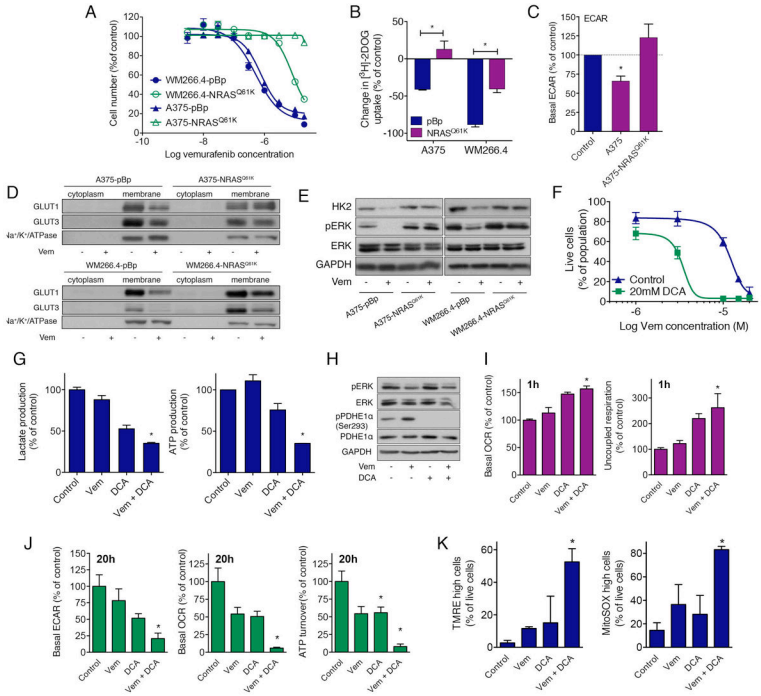

Figure 2.

NRAS-mediated resistance to vemurafenib (Vem) is associated with restored glycolysis and can be overcome by combination with a glycolysis inhibitor. **A** cell proliferation in melanoma cells transduced with empty vector (pBp) or activated NRAS ($NRAS^{Q61K}$) (0-10μM Vem; 72h) **B** [^{3}H]-2DOG uptake in pBp vs. $NRAS^{Q61K}$ $BRAF^{V600E}$ melanoma cells (Control vs. 10μM Vem; 20h). **C**, ECAR in pBp vs. $NRAS^{Q61K}$ human melanoma cells (% of control) determined using a Seahorse XF24 Extracellular Flux Analyzer. **D** membrane vs. cytoplasmic GLUT1 and GLUT3 expression in A375- and WM266.4-pBp vs. $NRAS^{Q61K}$ melanoma cells (Control vs 10μM (A375) or 3μM (WM266.4) Vem 20h). Cytoplasmic and membrane extracts were sequentially prepared from drug-treated cells and equal protein was used for Western immunoblotting Na^+K^+-ATPase was used as a membrane-specific loading control. **E** effect of Vem on protein expression in A375- and WM266.4-pBp vs. $NRAS^{Q61K}$ melanoma cells (Control vs 10μM (A375) or 3μM (WM266.4) Vem 20h) was determined by Western immunoblotting using GAPDH as a loading control. **F** cell survival (determined by Annexin-V/PI staining) in the presence of Vem or Vem + DCA in M249-AR4 melanoma cells (0-20μM Vem ± 20mM DCA; 72h). M249-AR4 Vem-resistant cells have been previously described and developed an $NRAS^{Q61K}$ mutation after long term selection in 1μM Vem. **G** effect of Vem + DCA on lactate and ATP production in M249-AR4 melanoma cells (0 vs. 15μM Vem ± 20mM DCA; 24h). **H** effect of Vem + DCA on protein expression in M249-AR4 melanoma cells (0 vs. 15μM Vem ± 20mM DCA; 24h). **I** basal OCR and uncoupled respiration (0 vs. 15μM Vem ± 20mM DCA; 1h) and **J** basal ECAR, OCR and ATP turnover (0 vs. 15μM Vem ± 20mM DCA; 20h) were determined in M249-AR4 melanoma cells. **K** mitochondrial membrane potential (72h) and ROS production (48h) were determined by FACS using TMRE and MitoSOX staining, respectively (0 vs. 15μM Vem ± 20mM DCA). **A-C, F, G, I-K** data

represent mean ± SEM (n=3). * $p<0.05$. **B** *t*-test correct for multiple comparisons using Holm-Sidak method. **C** two-way ANOVA coupled with Tukey's *post-hoc* test. **G, I-K** one-way ANOVA coupled with Tukey's multiple comparison *post-hoc* test. **D, E, H** images are representative of 2 independent experiments.

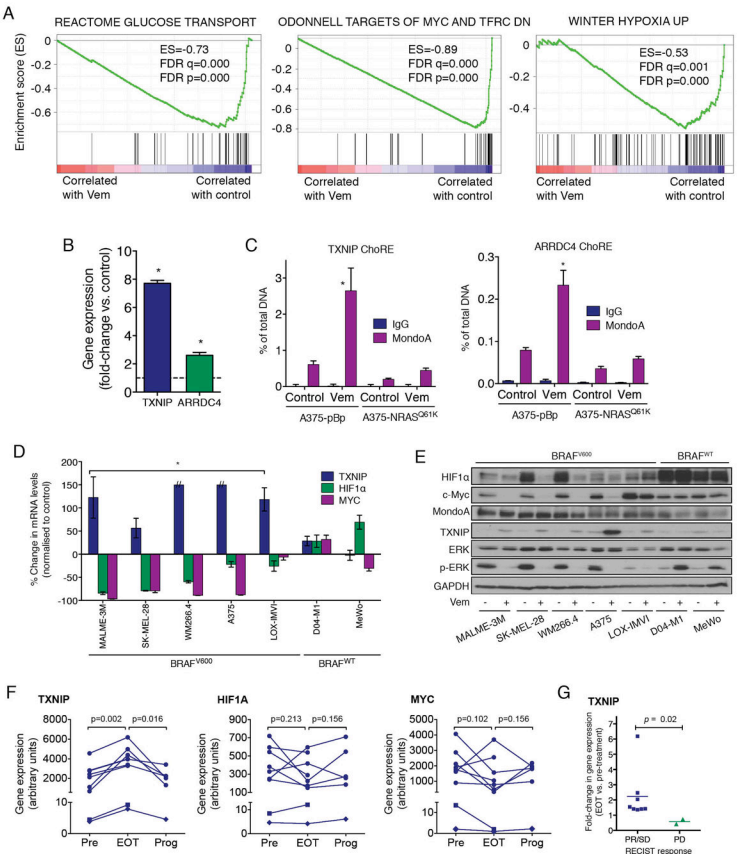

Figure 3.

BRAF^{V600} promotes HIF1α and c-Myc expression and suppresses MondoA expression in human melanoma cells. **A** effect of vemurafenib (Vem) on expression of a glucose transport gene set and expression of the top ranked c-Myc and hypoxia gene sets. A375 cells were treated with 0 vs. 3μM Vem for 24h (n=3) after which RNA was extracted and subjected to microarray analysis of gene expression. GSEA was performed on these data to determine significantly enriched gene sets in either control or drug treated cells. **B** effect of BRAF inhibition on mRNA expression or the MondoA targets, TXNIP and ARRDC4, in A375 melanoma cells (gene expression data from microarray experiments; Vehicle vs. 10μM Vem; 24h). **C** MondoA binding to the TXNIP and ARRDC4 promoters in BRAF^{V600} A375-pBp or A375-NRAS^{Q61K} cells (0 vs. 3μM Vem; 24h). **D** expression of TXNIP, ARRDC4, HIF1α and c-Myc mRNA in melanoma cells (0 vs. 3μM Vem; 20h). **E** protein expression/ phosphorylation in melanoma cells (Vehicle vs. 3μM Vem; 24h). **F** mRNA expression in melanoma biopsies. For patients 1-7 ((x025CF)),RNA was extracted from fresh-frozen BRAF^{V600} melanoma biopsies from patients pre-treatment (Pre), early on dabrafenib therapy (On; 140-600mg daily; biopsies take between day 3-14) and post-progression (Prog). Changes in gene expression were determined using an Illumina BeadStation (patients 1-7 (x025CF)), Affymetrix Human Gene 1.0 ST Arrays (patient 8 (x25C6)) or by RNAseq for patient 9 ((x025A0)). **B-D** each data point represents mean ± SEM (n=3) * p<0.05. **C** one-way ANOVA coupled with Tukey's *post-hoc* test. **D** data were analysed using *t*-tests **E** images are representative of 2 independent experiments. **F** Data points

represent mean data values across all biopsies from a single patient pre-treatment and lines represent individual patients. Data were analysed using *t*-tests coupled with Wilcoxon's matched-pairs signed rank test and $p<0.05$ denotes a statistically significant difference. **G** Lines represent mean fold-change in gene expression (EOT vs. Pre) and symbols represent individual patients. Data were analysed using a *t*-test coupled with a Mann-Whitney test where $p<0.05$ denotes a statistically significant difference.

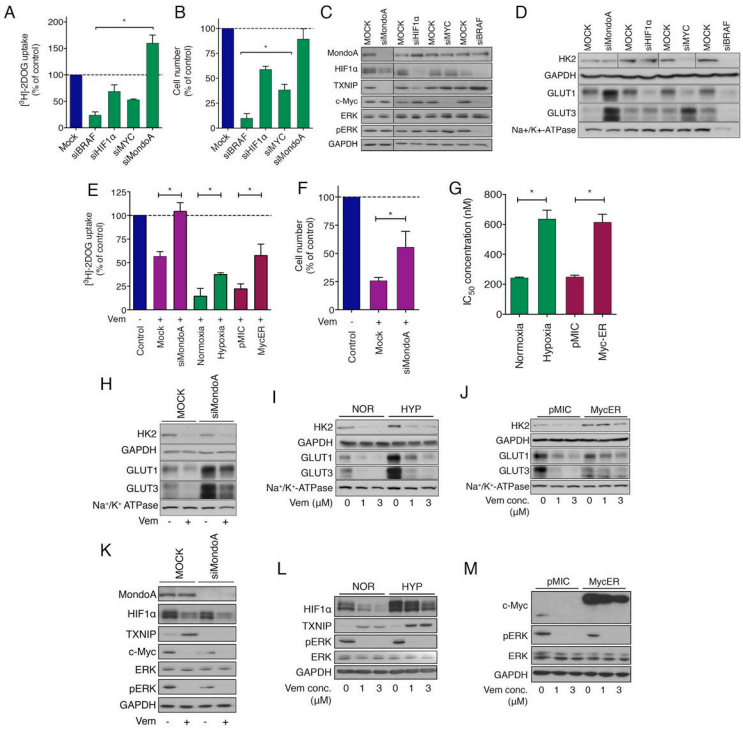

Figure 4.

MondoA, HIF1α and c-Myc regulate basal glucose uptake and cell proliferation in melanoma cells and participate in responses to BRAF inhibition. **A** [^{3}H]-2DOG uptake and **B** cell proliferation in WM266.4 melanoma cells after siRNA-mediated gene knockdown (Mock control vs. siRNA; 72h post-transfection). **C & D** protein expression in WM266.4 melanoma cells after siRNA-mediated gene knockdown (Mock control vs. siRNA; 72h post-transfection). **E** effect of vemurafenib (Vem) on [^{3}H]-2DOG uptake in WM266.4 melanoma cells after siRNA-mediated gene knockdown of mondoA (72h post-transfection; 0 vs. 1μM Vem, 8h), expression of inducible c-Myc (MycER; 0 vs. 3μM Vem, 16h) or exposure to hypoxia (2% oxygen; 0 vs. 3μM Vem, 16h). **F** effect of Vem on cell proliferation in WM266.4 melanoma cells ± siRNA-mediated gene knockdown of mondoA (72h post-transfection; 0 vs. 1μM Vem, 48h). **G** Vem sensitivity (proliferation IC50s) after expression of inducible c-Myc (MycER) or exposure to hypoxia (2% oxygen; 0-10μM Vem, 72h). **H-M** effect of Vem on protein expression in WM266.4 melanoma cells after siRNA-mediated gene knockdown of mondoA (72h post-transfection; 0 vs. 1μM Vem, 8h), expression of inducible c-Myc (MycER; 0, 1 or 3μM Vem, 16h) or exposure to hypoxia (2% oxygen; 0, 1 or 3μM Vem, 16h). **A, B, E-G** data represent mean ± SEM (n=3). * p<0.05. **A, B, G** data were analysed using *t* -tests. **E, F** two-way ANOVA coupled with Tukey's *post-hoc* test. **C, D & H-M** images are representative of 2 independent experiments.